



Technical Sciences
Academy of Romania
www.jesi.astr.ro

Received 4 November 2024

Accepted 10 March 2025

Received in revised form 30 January 2025

Thermal shock behavior of Cr₂O₃ - based plasma sprayed coatings

**DANIEL CRISTISOR¹, DANIELA-LUCIA CHICET¹
BOGDAN ISTRATE¹, CORNELIU MUNTEANU^{1,2*}, FABIAN LUPU¹**

¹*Gheorghe Asachi Technical University of Iasi, Blvd. Mangeron, No. 61, 700050, Iasi, Romania.*

²*Technical Sciences Academy of Romania*

Abstract. Atmospheric Plasma Spray (APS) coatings have earned a well-deserved place in the category of thermal spray coatings over the last decades, as they have brought coatings made of ceramic materials to the forefront. This has greatly extended the range of applications of these coatings, ranging from improved wear resistance to enhanced resistance to use at very high temperatures. In this study it is analyzed how two thermally sprayed Cr₂O₃-based coatings, a 99wt% Cr₂O₃ powder and a Cr₂O₃-10wt%TiO₂ powder, were affected by exposure to thermal shock, with temperatures recorded in the range of 700 to 900°C. The samples were analyzed by scanning electron microscopy and EDS analysis (Energy Dispersive Spectroscopy), the results being completed by roughness measurements on the affected areas using a Mahr perthometer and AFM (Atomic Force Microscopy). No major changes were observed in the comparative behavior of the two coatings, nor in comparison with the material not affected by thermal shock, both in terms of morphology and chemical composition of the areas subjected to thermal shock, as well as their roughness or compactness. It can thus be concluded that the presence of a small percentage of TiO₂ does not negatively influence the thermal shock behavior of this type of coating, and the range of applications can be extended to high temperatures.

Keyword: plasma spray, thermal shock, chromium oxide, coating morphology.

1. Introduction

One of the effective ways to improve the mechanical, physical and chemical properties is to modify material characteristics in the surface area, rather than modifying the entire material mass. Thus, through surface engineering, the service life can be extended by improving the mechanical characteristics of resistance to

*Correspondence address: munteanu@tuiasi.ro

fatigue, wear, friction, or the physical, chemical and thermal characteristics of resistance to corrosion and high temperatures.

Surface engineering has a multitude of methods available for modifying interfaces, either by layer transformation with microstructure modification, or by coating with various types of layers, physicochemically or mechanically bonded to the substrate [1]. One method that has gained a lot of ground in the last decades is the deposition of thermal spray coatings [2]. This method is characterized by the formation of a coating with a lamellar structure that can have thicknesses ranging from 50 microns to a few millimeters and can be made of both metallic, but also ceramic or ceramometallic materials, single or combined in several successive layers [3].

One such layer is that obtained from a chromium oxide ceramic matrix, which can be deposited as such or combined with various other ceramic and/or metallic materials [4]. Cr₂O₃ coatings have found numerous industrial applications over time, such as the protection of surfaces exposed to severe working conditions in the aerospace, energy, automotive, chemical and even food industries [5].

One of the most common applications is the protection against abrasive wear and erosion, even in abrasive fluids (slurry erosion). Cr₂O₃ coatings are used in high-performance equipment such as press rollers in the printing industry, components subject to intense friction such as pistons and cylinders in internal combustion engines and in the aerospace industry [6, 7], providing effective protection and prolonging their service life. These coatings have high wear resistance due to their high hardness (above 1600 HV) as well as low coefficient of friction. A study [8] on the erosion behavior of Cr₂O₃ layer applied on martensitic steel (AISI 410) showed that the impact angle of the eroding particles significantly influences the wear resistance, even at impact angles of 60° and 75°, compared to lower angles. In highly demanding industrial environments, such as mining facilities and hydropower equipment, Cr₂O₃ coatings applied on metallic substrates protect against erosion and abrasion caused by suspended solid particles, an example being the study on Cr₂O₃ coatings deposited on AISI 410 steel that provided superior resistance compared to uncoated substrates [9].

Cr₂O₃ coatings are also known for their excellent corrosion resistance, which makes them suitable for applications where components are exposed to aggressive chemical or saline environments, such as turbines, pumps, chemical processing equipment or those in the food industry [10, 11]. These dense, hard coatings act as a protective barrier, preventing corrosive agents from penetrating the metal substrate.

Another use of these coatings is for applications where materials are subjected to high temperatures due to their thermal stability and resistance to oxidation. These coatings are applied on components in gas turbines and power generation equipment to prevent degradation caused by extreme temperatures and eroding particles [7, 9], and have been shown to outperform other oxides, such as Al₂O₃, due to its chemical stability and oxidation resistance.

In tribological property testing, Cr₂O₃ coatings demonstrated excellent performance in reducing friction and wear in both dry and wet contact. In addition, the

introduction of oxide additions, such as TiO_2 and Al_2O_3 , can modify the tribological properties and microstructure of the coating, improving wear resistance and hardness, so that $\text{Cr}_2\text{O}_3\text{-TiO}_2$ and $\text{Cr}_2\text{O}_3\text{-Al}_2\text{O}_3$ coatings exhibit higher wear resistance in intense friction applications and provide high stability in high temperature environments and intense mechanical loads [12 - 14].

A disadvantage of Cr_2O_3 coatings is their local brittleness, which manifests itself especially if they are subjected to very high local pressures during use [15], which generate macro-cracks and implicitly the destruction of the coating. A method to diminish this undesirable characteristic is the addition of oxides in the flow of spray material, such as Al_2O_3 [16], TiO_2 [17], ZrO_2 [7], BaCrO_4 [18] or SiO_2 [19], both individually and in complex combinations. Their addition in small percentages (less than 5%wt) has the effect of forming glassy phases with low melting point, to increase the adhesion between the lamellae in the deposited layer without changing the intrinsic characteristics of the Cr_2O_3 [7] matrix. Several low alloyed powders with TiO_2 , ZrO_2 [7], SiO_2 [24], or combinations thereof have already become commercial materials (13). A series of nanostructured Cr_2O_3 - Ag nanostructured coatings [20] are currently being tested to improve the structural characteristics and mechanical properties, and both the mechanisms of high temperature formation of the lubricant film on NiCoCrAlY - Cr_2O_3 - AgMo coatings [21] and the effect of graphite addition [22] are being studied to improve the tribological characteristics.

According to the studies available in the literature, titanium oxide (TiO_2) can significantly improve the properties of chromium oxide (Cr_2O_3) coatings made by thermal spraying, influencing several key aspects related to mechanical strength, wear resistance and tribological behavior. In terms of toughness improvement and porosity reduction, TiO_2 contributes to reduce the porosity of Cr_2O_3 coatings and increase their density. This combination leads to improved mechanical strength and a more uniform particle distribution [22, 23]. In particular, the addition of TiO_2 helps to reduce microcracking and improves the ability to withstand high mechanical loads [19, 24]. Other studies have shown that the inclusion of TiO_2 in Cr_2O_3 coatings improves wear and erosion resistance by reducing the tendency to microcracking and improving toughness [23, 24]. For example, $\text{Cr}_2\text{O}_3\text{-25\%TiO}_2$ coatings have higher abrasion resistance, which makes them more suitable for applications in demanding environments such as industrial equipment [7, 22].

TiO_2 also acts as a solid lubricant in Cr_2O_3 matrix coatings, which leads to a decrease in the coefficient of friction and improved tribological behavior under severe friction conditions [22, 24]. Another advantage of $\text{Cr}_2\text{O}_3\text{-TiO}_2$ -based coatings is that they exhibit superior thermal stability of the constituent phases at elevated temperatures, as TiO_2 intervenes in the formation of a stable solid solution in the crystalline structure of Cr_2O_3 , thus preventing degradation of the material [7, 23], which can thus be used in applications involving exposure to high temperatures. In corrosive environments, $\text{Cr}_2\text{O}_3\text{-TiO}_2$ coatings exhibit superior corrosion resistance compared to that of a coating made solely of Cr_2O_3 , due to its denser structure and its protective properties against oxidation [19].

In this study, it was observed how two thermally sprayed Cr₂O₃-based coatings, a Cr₂O₃ powder (99wt%) and a Cr₂O₃-10wt%TiO₂ powder, were affected by exposure to thermal shock, with temperatures recorded in the range of 700 to 900°C. The thermal shock was obtained by heating-cooling cycles exposure in a 2kw MSSf vertical axis solar furnace in the PROMES / CNRS laboratory in Odeillo - Font Romeu France. The samples were analyzed by scanning electron microscopy and EDS analysis (Energy Dispersive Spectroscopy), the results being completed by roughness measurements on the affected areas using a Mahr Perthometer and AFM (Atomic Force Microscopy).

2. Experiment

2.1. Materials and methods used for APS coatings

In order to study how the TiO₂ alloying percentage influences the microstructure of a plasma-spray deposited (APS) Cr₂O₃-based matrix coating, two commercially available powders were purchased from the market: Amdry 6415 (99%wt Cr₂O₃, melt sintered and ground) and Metco 6483 (40%wtTiO₂, mixed). To modify the alloying percentage, the amounts required to obtain 10wt% TiO₂ alloying by mechanically mixing Cr₂O₃ powder with Cr₂O₃-40%wtTiO₂ powder were calculated and measured by weighing on an electronic balance [25]. The nominal particle size distributions are (- 15 +5) µm for Cr₂O₃ powder and (- 90 +16) µm for Cr₂O₃-40%wt%wt TiO₂, both with an angular polygonal morphology.

The SprayWizard 9MCE (Metco - Oerlikon, 2006) was used for thermal spraying, with the following parameters: voltage - 58.8 V, current - 496 A, primary gas flow (argon) - 60 NLPM, secondary gas flow (hydrogen) - 45 NLPM, powder feed rate. The substrate is low alloy steel (max.0.17%C, max. 1.4%Mn, max. 0.035%P, max. 0.035%S, max. 0.12%N, max. 0.55%Cu, according to EN 10025-2/2004), with a rectangular geometry (60 x 30 x 5 mm) and rounded corners. The surface of each sample was prepared by sandblasting with quartz sand in order to clean all the impurities and activate it by texturizing. To ensure the reproducibility of the experiment, three samples of each type of coating were produced.

2.2. Materials and methods used for thermal shock study

The study of the thermal shock behaviour of the analysed coatings was carried out using a vertical axis solar furnace in the PROMES / CNRS Laboratory in Odeillo-Font Romeu France, by heating-cooling cycles exposure in a 2kw MSSf vertical axis solar furnace.

The samples were subjected in turn to heating-cooling cycles at temperatures between 800 and 900°C, cooling being carried out with a jet of compressed air blown over the heated area. The temperature was recorded using a K-type thermocouple, some aspects during the tests being presented in Figure 3 a) - d). Figure 3 a) shows how the sample was mounted and the positioning of the K

thermocouple, which was connected to the Graphitec reader, that sequentially records the graph of the temperature variation over time (see Figure 4). Figure 3 b) shows the positioning of the sample under the concentrator. After that, a position of maximum concentration of solar radiation was obtained in an area higher than the sample surface, which was descended and stabilised on the sample surface (Figure 3 c). The thermal shock was obtained by periodically blowing jets of compressed air on the surface subjected to solar radiation, while blocking the heating.

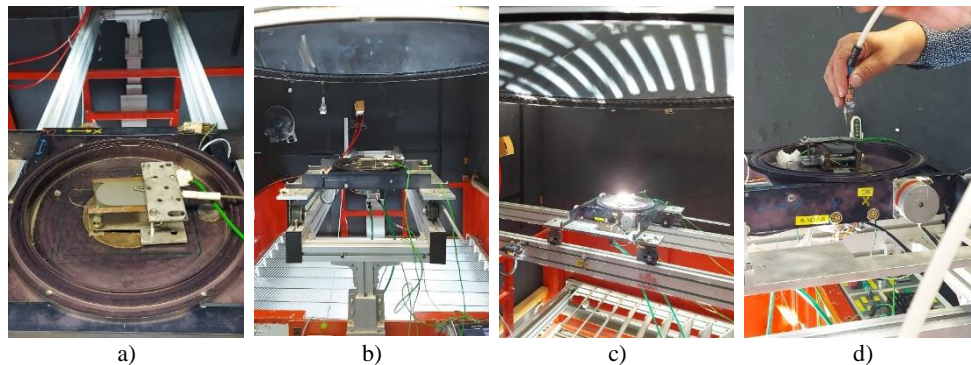


Fig. 3. Aspects during thermal shock tests: a) mounting of the sample and positioning of the K thermocouple, b) positioning of the sample under the solar concentrator, c) moment of positioning the focusing zone on the sample, d) forced cooling operation with compressed air for the thermal shock.

Figure 4 shows the 2 graphs generated during the heat shock tests for tested samples. The red line shows the temperature variation of the ceramic layer and the black line shows the temperature variation of the substrate.

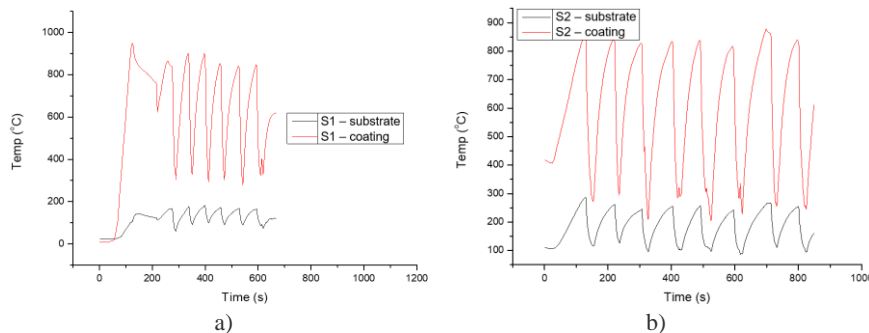


Fig. 4. Temperature variation graphs recorded during the thermal shock tests of: a) S1; b) S2.

It is observed that the temperature variations in the deposited layer are echoed in the substrate, but the temperature amplitude is small, which means that the substrate is not affected by major structural transformations.

The equipment used for the characterization of the layers subjected to thermal shock was the Vega Tescan II Scanning Electron Microscope and the EDS Detector produced by Bruker. An additional analysis of the surface roughness was

performed using Mahr Perthometer and Nanosurf Easy Scan 2 for Atomic Force Microscopy analysis.

3. Results and discussion

3.1. SEM and EDS analysis of the S1 coatings (99%wt Cr₂O₃)

In the case of sample 1, it can be seen that no morphological change of the coatings occurs as shown in Figure 5, and the specific porous appearance of the thermal spray coatings is unchanged. However, a visible difference was observed in the form of color change ("staining") on the heat-affected area.

The elemental chemical analysis of the areas of interest did not show the presence of other elements, the distribution of Cr, O and C being uniform and unchanged compared to the initial reference area, as shown in Figures 6 and 7.

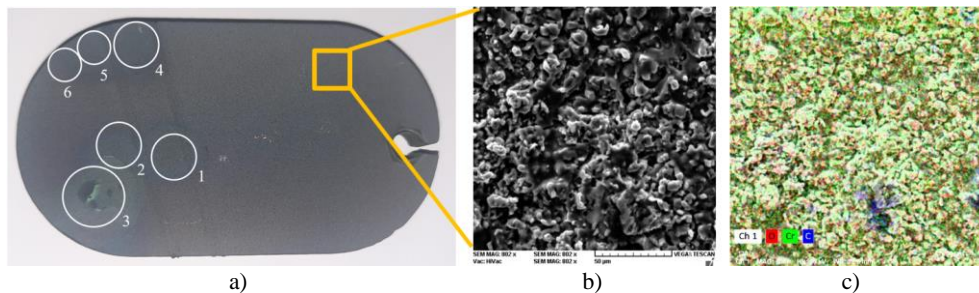


Fig. 5. The general aspect of sample 1 with areas subjected to thermal shock. Area of interest no.1: average temperature 800°C, 9 cycles/10 seconds

Fig. 6. Images of secondary electrons at 800 x(a) and EDS map at 500 x (b) on the reference surface of sample S1.

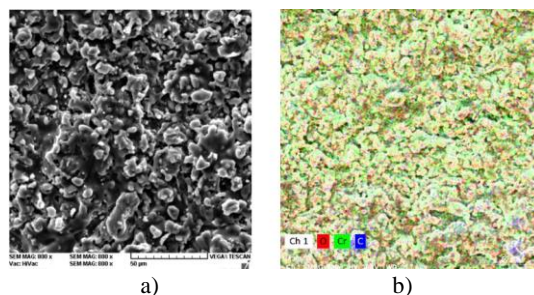


Fig. 7. Images of secondary electrons at 800x (a) and EDS map at 500x (b) on the thermal shock surface (area 1) of sample S1.

3.2. SEM and EDS analysis of the S2 coatings (Cr₂O₃ - 10%wt TiO₂)

It can be seen that also in the case of sample 2 there were no changes in the morphology of the coating (e.g. local melting, oxidation with formation of oxide products, cracking) regardless of the temperature or cycles applied, as shown in the

Figures 8, 9 and 10. The same conclusion is supported by the distribution maps on the areas subjected to thermal shock, which show a uniform distribution of the component elements compared to the reference surface. The only changes, also in this case, are the darker patches on the heated areas, observed by visual analysis.

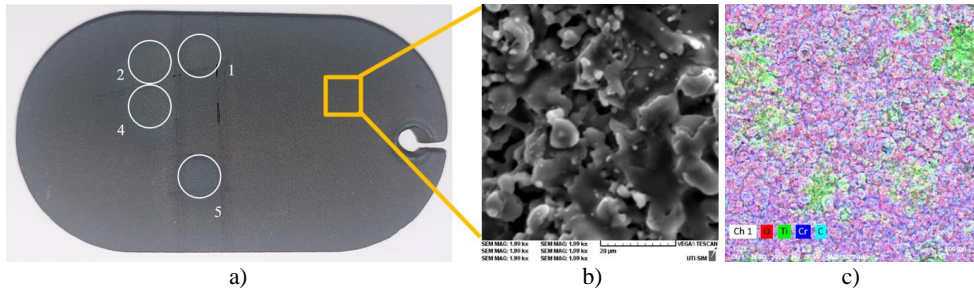


Fig. 8. The general aspect of sample 2 with areas subjected to thermal shock. Area of interest no.4: average temperature 800°C, 9 cycles/10 seconds

Fig. 9. Images of secondary electrons at 2000x (a) and EDS map at 200x (b) on the reference surface of sample S2.

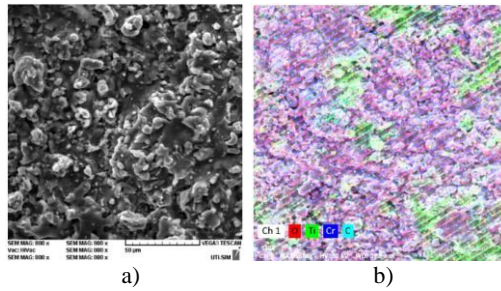


Fig. 10. Images of secondary electrons at 800x (a) and EDS map at 500x(b) on the thermal shock surface (area 4) of sample S2.

3.3. Comparative EDS analysis of the coatings after thermal shock

For an assessment of the degree of oxidation, the weight percentages of the chemical elements present in the areas subjected to thermal shock were comparatively analyzed and the values obtained are summarised in Table 1.

Table 1. Variation of the chemical elements percentage on the interest area of the samples subjected to thermal shock

Sample	Area	%wt Cr	%wt O	%wt Ti	%wt C
S1 (99 wt% Cr₂O₃)					
Reference	0	62.860	33.070	-	4.060
800°C, 9 cycles x 10 sec.	1	64.760	32.930	-	2.300
S2 (Cr₂O₃ + 10 wt% TiO₂)					
Reference	0	49.930	38.940	8.610	2.520
800°C, 9 cycles x 10 sec.	4	49.340	39.430	7.660	3.570

It can be seen that there are no dramatic increases in the percentages of oxygen in any of the thermal shock areas compared to the reference areas (those on which no heat shock or heating was applied), so no additional oxidation of the layer occurs, regardless of the temperature at which it was heated.

However, there is a variation in the mass percentage of the chemical elements proportional to the change in the TiO₂ alloying percentage (as expected), namely: a decrease in the percentage of Cr with increasing TiO₂ alloying percentage and an increase in the percentages of Ti and O with increasing TiO₂ alloying percentage. A decrease in the percentage of C with increasing TiO₂ alloying is also observed.

3.4. Surface roughness evaluation after thermal shock – Mahr Perthometer

The surfaces of the areas subjected to thermal shock were also analyzed in terms of roughness variation, on each of the areas of interest, using a Mahr-type Perthometer. Three measurements were made for each area, the length of the route being the same for each case: Lt = 5.6 mm. The averaged values are summarised in Table 2.

When comparing the areas of each sample with the reference surface, no relevant changes in their roughness are observed. Also, when comparing the 2 types of coatings, it is observed that Ra increases slightly with increasing of the TiO₂ alloying percentage.

Table 2. Average values of the roughness of the interest areas of the samples subjected to thermal shock

Sample	Area	Ra (avg) [μm]	Rz (avg) [μm]	Rmax (avg) [μm]	Pc (avg) [cm ⁻¹]
S1 (99 wt% Cr₂O₃)					
Reference	0	3.342	20.467	24.533	130.000
800°C, 9 cycles x 10 sec.	1	3.430	19.550	24.350	133.000
S2 (Cr₂O₃ + 10 wt% TiO₂)					
Reference	0	4.419	27.400	37.167	86.000
800°C, 9 cycles x 10 sec.	4	3.830	24.400	32.250	124.000

3.5. Surface roughness evaluation of the coatings after thermal shock (AFM)

Atomic force microscopy analysis was used for in-depth analysis of the influence of thermal shock on surface roughness at a micrometric scale, and thus on the structural transformations that might occur when thermal shock is applied.

For this reason, two surfaces were scanned on the areas of interest of sample 1, both on the reference surface (Figure 11) and on the surface affected by the thermal shock (Figure 12).

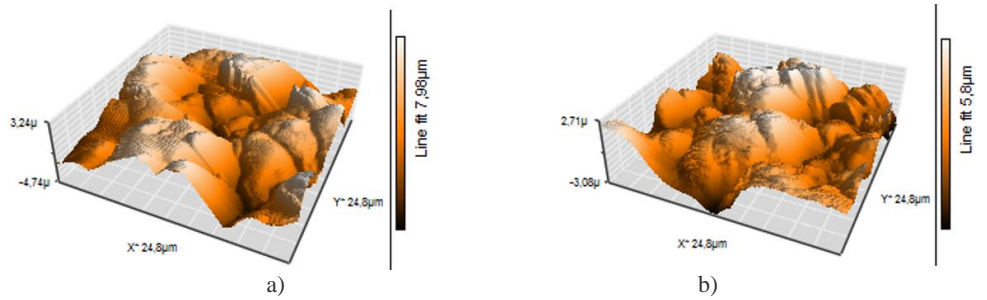


Fig. 11. 3D representations of the reference surface of sample 1: position 1 (a) and position 2 (b).

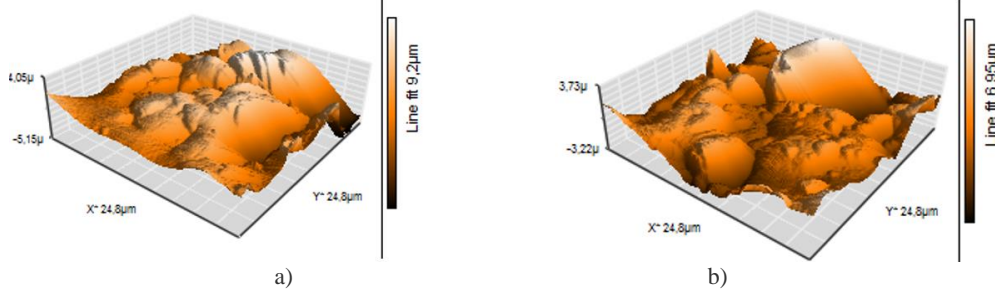


Fig. 12. 3D representations of thermal shock area no.1 from S1: position 1 (a) and position 2. (b).

Table 4. Roughness average values of the AFM scanned surfaces, from sample 1.

Sample	Area [μm^2]	Sa [nm]	Sq [nm]	Sm [μm]
S1 (99 wt% Cr₂O₃)				
Reference (1)	618	1194.9	1408.9	342.99
Reference (2)	618	919.61	1153.1	245.63
800°C, 9 cycles x 10 sec (1)	618	1239.5	1561.8	88.043
800°C, 9 cycles x 10 sec (2)	618	872.64	1114.1	273.17

In the resulting graphs, the irregular surface specific to thermal spray coatings can be seen. In the attached table (Table 4) the average values of the roughness of the scanned surface are presented, and it is observed that there is no clear trend of influence of the thermal shock application on the surface quality, at this scale.

The same observations were made for sample 2, as presented in Figures 13 and 14, so we cannot yet make clear comments on how the presence of TiO₂ influences the surface appearance of the samples before and after heat shock application.

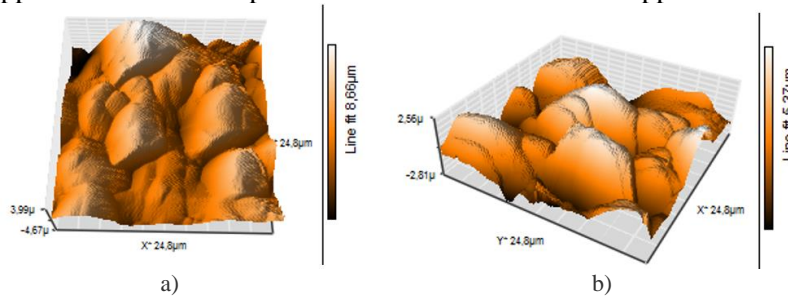


Fig. 13. 3D representations of the reference surface of S2: position 1 (a) and position 2 (b).

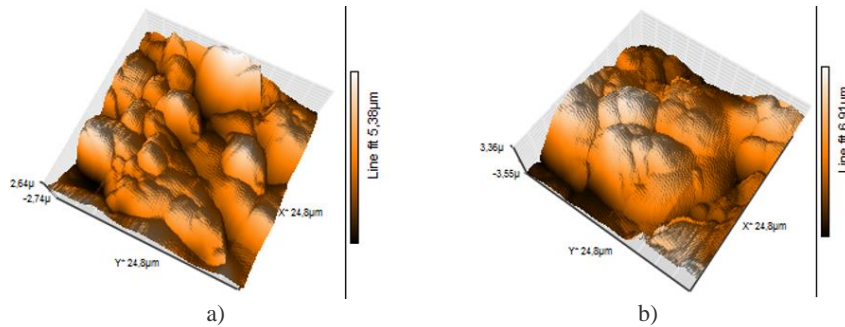


Fig. 14. 3D representations of thermal shock area no.4 from S2: position 1 (a) and position 2. (b).
Table 5. Roughness average values of the AFM scanned surfaces, from sample 2.

Sample	Area [μm^2]	Sa [nm]	Sq [nm]	Sm [μm]
S2 (Cr₂O₃ + 10 wt% TiO₂)				
Reference (1)	618	1075.3	1368.4	276.91
Reference (2)	618	868.41	1069.5	426.23
800°C, 9 cycles x 10 sec (1)	618	1190.9	1432.2	56.942
800°C, 9 cycles x 10 sec (2)	618	705.13	884.15	202

4. Conclusions

Thermal spraying is a versatile process and plays a key role in improving material performance and reducing long-term costs. With a wide range of applications and adaptability to diverse industries, this technology supports advances in energy efficiency and sustainability and is a critical component for modern technological and industrial development.

Morphological analysis of the coatings revealed no major defects on the surface or at the interface with the substrate, the overall appearance being uniform, without discontinuities or macro cracks.

The Ti element is mainly present in splat-type areas, which confirms the role of finishing the structure, i.e. increasing the ductility of the ceramic coatings of which TiO₂ powder is part, by increasing the degree of incorporation of semi-molten or non-molten particles and by increasing the adhesion between the splats formed during spraying.

In the thermal shock tests, it was observed that in none of the cases did the morphology of the coating change (local melting, oxidation with formation of oxide products, cracking) irrespective of the temperature or cycles applied.

There are no dramatic increases in oxygen percentages in any of the heat-affected areas compared to the reference areas, so there is no additional oxidation of the coating regardless of the temperature at which it was heated.

When comparing the roughness of the areas on each sample with the reference surface, no relevant changes in roughness are observed. Also, when comparing the 2 types of coatings, it is observed that Ra increases slightly with increasing TiO₂ alloying percentage.

Acknowledgements.

A part of the paper has received funding from the European Union's Horizon 2020 research and innovation programme under grant agreement No 823802. We thank the CNRS-PROMES laboratory, UPR 8521, for providing access to its installations, the support of its scientific and technical staff, within this grant agreement No 823802 (SFERA-III), SURPF2301300009, Ceramic layers as thermal barriers for aircraft turbine engines, CeLaTeBa.

References

- [1] Toma S.L., Chicet D.L., Cazac A.M., *Numerical Calculation of the Arc-Sprayed Particles' Temperature in Transient Thermal Field*, Coatings, **12**, 7, 877, 2022.
- [2] Chicet D., Tufescu A., Paulin C., Panturu M., Munteanu C., *The Simulation of Point Contact Stress State for APS Coatings*, IOP Conference Series: Materials Science and Engineering, **1**, 209, 2017, art. no. 012044.
- [3] Daniel Cristişor, Daniela Lucia Chicet, Cornelia Paleu, Cristian Stescu, Corneliu Munteanu, *Substrate Texture Influence on the Dry Sliding Wear Behavior of WC-CoNiCr Plasma Spray Coating*, Archives Of Metallurgy And Materials, **68**, 3, 2023, p. 1061 – 1067.
- [4] Xiong Yang, Shujuan Dong, Jinyan Zeng, Xin Zhou, Jianing Jiang, Longhui Deng, Xueqiang Cao, *Sliding wear characteristics of plasma-sprayed Cr₂O₃ coatings with incorporation of metals and ceramics*, Ceramics International, **45**, 2019, p. 20243 – 20250.
- [5] Odhiambo John Gerald, Li Wenge, Zhao Yuan Tao, Li Cheng Long, Li Qiang, *Influence of plasma spraying current on the microstructural characteristics and tribological behaviour of plasma sprayed Cr₂O₃ coating*, Boletín de la sociedad española de cerámica y vidrio, **60**, 2021, p. 338–346.
- [6] Bayram Benli, Ilhan Celik, *Surface Modification and Analysis of St37 Steel with Al₂O₃-TiO₂, ZrO₂, and Cr₂O₃ Ceramic Coatings: Structural, Mechanical, and Tribological Properties*, Tribology International, **191**, 2024.
- [7] Giovanni Bolelli, Daniel Steduto, Jarkko Kiilakoski, Tommi Varis, Luca Lusvarghi, Petri Vuoristo, *Tribological properties of plasma sprayed Cr₂O₃, Cr₂O₃-TiO₂, Cr₂O₃-Al₂O₃ and Cr₂O₃-ZrO₂ coatings*, Wear, 203931, 2021, p. 480 – 481
- [8] Sreenivas Rao K.V., Girisha K.G., Sushruta Eswar, *Effect of Eroding Impact Angle on the Erosion Behaviour of Plasma Sprayed Cr₂O₃ coating on Martensitic steel*, Materials Today: Proceedings, **4**, 2017, p. 10221–10224
- [9] Sreenivasa Rao K.V., Ramesh C.S., Girisha K.G., Rakesh Y.D., *Slurry Erosive Wear Behavior of Plasma Sprayed Cr₂O₃ Coatings on Steel Substrates*, Materials Today: Proceedings, **4**, 2017, p. 10283–10287.
- [10] Pejman Zamani, Zia Valefi, Kouros Jafarzadeh, *Comprehensive study on corrosion protection properties of Al₂O₃, Cr₂O₃ and Al₂O₃-Cr₂O₃ ceramic coatings deposited by plasma spraying on carbon steel*, Ceramics International, **48**, 2022, p. 1574 – 1588.
- [11] Sreenivasa Rao K.V., Girisha K.G., Anjan S, Abhilash Sharma N., *Experimental Investigation of Corrosion Behavior of Plasma Sprayed Cr₂O₃ Coatings on 410 grade Steel*, Materials Today: Proceedings, **4**, 2017, p. 10254–10258
- [12] Xiong Yang, Jinyan Zeng, Hao Zhang, Jinshuang Wang, Junbin Sun, Shujuan Dong, Jianing Jiang, Longhui Deng, Xin Zhou, Xueqiang Cao, *Correlation between microstructure, chemical components and tribological properties of plasma-sprayed Cr₂O₃-based coatings*, Ceramics International, **44**, 2018, p. 10154 – 10168.
- [13] Hakan Cetinel, Erdal Celik, Murat I. Kusoglu, *Tribological behavior of Cr₂O₃ coatings as bearing materials*, Journal of Materials Processing Technology, **196**, 2008, p. 259–265.
- [14] Madhu Sudana Reddy, C Durga Prasad, Pradeep Patil, M.R. Rameshd, Nageswara Rao, *Hot corrosion behavior of plasma-sprayed NiCrAlY/TiO₂ and NiCrAlY/Cr₂O₃/YSZ cermets coatings on alloy steel*, Surfaces and Interfaces, **22**, 2021, 100810.

- [15] Y. Xie, H. Hawthorne, *The damage mechanisms of several plasma-sprayed ceramic coatings in controlled scratching*, *Wear*, 233–235, 1999, p. 293–305.
- [16] Setu Suman, Kazi Sabiruddin, *Behavior of free – standing atmospheric plasma sprayed Al₂O₃ – Cr₂O₃ solid solution – based coatings under cyclic heating at 1000°C*, *Surface & Coatings Technology*, **490**, 2024, 131180.
- [17] Angelos Koutsomichalis, Antonios Lontos, George Loukas, Michalis Vardavoulias and Nikolaos Vaxevanidis, *Fatigue behaviour of Plasma Sprayed Titania and Chromia Coatings*, MATEC Web of Conference, **349**, 02009, 2021, ICEAF-VI 2021.
- [18] Weiming Su, Shaopeng Niu, Yicong Huang, Chao Wang, Yuyin Wen, Xin Li, Chunming Deng, Changguang Deng, Min Liu, *Friction and wear properties of plasma-sprayed Cr₂O₃–BaCrO₄ coating at elevated temperatures*, *Ceramics International*, **48**, 2022, p. 8696 – 8705.
- [19] Hao Zhang, Yongjun Wang, Xiangxiang Chen, Zhengzheng Zhang, Xian Zeng, Xudong Chen, *Corrosion behaviors of Al₂O₃–20TiO₂ and Cr₂O₃–3TiO₂–5SiO₂ coatings in both artificial seawater and high-pressure hydrogen sulfide seawater*, *Ceramics International*, **50**, 2024, p. 34346 – 34356.
- [20] Ehsan Sadri, Fakhreddin Ashrafizadeh, *Structural characterization and mechanical properties of plasma sprayed nanostructured Cr₂O₃-Ag composite coatings*, *Surface & Coatings Technology*, **236**, 2013, p. 91–101.
- [21] Tiantian Zhang, HaoLan, Chuanbing Huang, Lingzhong Du, Weigang Zhang, *Formation mechanism of the lubrication film on the plasma sprayed NiCoCrAlY- Cr₂O₃-AgMo coating at high temperatures*, *Surface & Coatings Technology*, **319**, 2017, p. 47–54.
- [22] Pranay Bagde, Sanket Mehar, SG Sapate, Avishkar Rathod, *Effect of graphite addition on tribological behavior of plasma sprayed Cr₂O₃-TiO₂ coating*, *Materials Today: Proceedings*, **56**, 2022, p. 2365–2370.
- [23] Han Hu, Lin Mao, Jinkun Xiao, Guodong Sun, Hanlin Liao, Chao Zhang, *Effect of hydrogen flow rate on microstructure and tribological properties of plasma-sprayed Cr₂O₃-65%TiO₂ composite coatings*, *Tribology International*, **189**, 2023, 108939.
- [24] Vinay Pratap Singh, Anjan Sil, Jayaganthan R., *Tribological behavior of plasma sprayed Cr₂O₃–3%TiO₂ coatings*, *Wear*, **272**, 2011, p. 149– 158.
- [25] Cristisor D., Chicet D.-L., Istrate B., Stescu C., Munteanu C., *Influence of TiO₂ Alloying Percentage on the Morphology of APS-deposited coatings from Cr₂O₃ Powders*, *Arch. Metall. Mater.*, **69**, 3, 2024, p. 1231-1239.